Fan W et al. Supplemental Figure legends

Supplemental Fig 1.

a, Insulin-induced FoxO1 phosphorylation in HIRC-B cells. HIRC-B cells were transfected with either control vector or pcDNA-FLAG-mFoxO1. The cells were starved overnight and subsequently treated with 100ng/ml insulin for 30'. Phosphorylated (p-256) and total FoxO1 were detected by western blotting. *b*, HIRc-B cells were co-transfected as described in Fig 1B, except that pcDNA-hPPARγ*2* was absent. Cells were then exposed to rosiglitazone or DMSO control before luciferase assay. Notice that neither FoxO1-WT nor FoxO1-CA had any effect on AOX-Luc promoter activity in the absence of PPARγ. *c*. HIRc-B cells growing in 24-well plates were co-transfected with 100 ng of FLAG-FoxO1 or pcDNA-FLAG control together with 200 ng of AOX-Luc, 5 ng of TK-β-Gal and 100 ng of pCMX-PPARα. Cells were treated with 1μM of specific PPARα ligand Wy14643 or DMSO control. *d*. The effect of FoxO1 on PPARβ/δ transactivation on AOX-Luc was studied in the presence of 0.1μM specific PPARβ/δ ligand GW501516. *e*. D10 3T3-L1 adipocytes were infected with adenovirus encoding either wild type FoxO1 or GFP control. Cells were starved in 0.1% BSA DMEM medium for 8 hours, followed by overnight incubation with 1μM

Rosiglitazone or DMSO control in combination with 100 ng/ml insulin or PBS Endogenous expression of *Hsp*47 mRNA was assayed by real-time time PCR. ROSI, Rosiglitazone; INS, insulin. Data are presented as the average ± SD. Letters above the bars show statistical groups (ANOVA, $p < 0.05$).

Supplemental Fig 2.

a, FoxO1 mRNA expression in adipocytes 48 hours post-electroporation with either control (siLuc) or anti-FoxO1 (siFoxO1) siRNA. *b*, Construction and validation of lentiviral short hairpin RNA against mouse FoxO1 (shFoxO1). A schematic representation of the short hairpin RNA (shRNA) lentiviral vector and the oligonucleotide sequences for constructing shFoxO1 lentivirus are shown. To validate the effectiveness of the shRNA construct, HEK293 cells were co-transfected with pcDNA-FLAG-FoxO1 together with one of four colonies of shFoxO1 plasmids. A ready-made shRNA construct against luciferase was used as a control. Two days after transfection, cells were lysed and blotted for FoxO1. SIN-LTR, self-inactivating long terminal repeat; Ψ, packaging signal; cPPT, central polypurine track; MCS, multiple cloning site; CMV, cytomegalovirus promoter; WRE, woodchuck hepatitis virus response element. *c*, Endogenous FoxO1 mRNA in mature 3T3-L1 adipocytes stably

expressing shFoxO1. *d*, Stable 3T3-L1 pre-adipocytes were established by transduction with lentivirus encoding shFoxO1, followed by two subsequent rounds of GFP+ sorting. The cells were then differentiated to mature adipocytes. On day 10, the cells were starved, and exposed to Rosiglitazone or DMSO, in the presence or absence of insulin, as indicated. *Pepck* mRNA was then assayed by real-time PCR. Data are presented as the average ± SD. Letters above the bars show statistical groups (ANOVA, $p < 0.05$).

Supplemental Fig 3.

a, Coimmunoprecipitation of endogenous PPARγ with FoxO1 in mature 3T3-L1 adipocytes. Cells were treated with INS(100 ng/mL), ROSI (1μM) or both as described in Fig 3A. Cell extracts were precipitated with anti-PPARγ antibody and then immunoblotted with anti-FoxO1 antibody. *b*, Modified one-hybrid assays. HIRc-B cells were co-transfected with 200 ng of Aox-Luc, 5 ng of TK-β-Gal and 100 ng of pcDNA-hPPARγ2. Vectors for FoxO1 (pcDNA-FLAG-FoxO1) or a VP16-FoxO1 fusion protein (either pACT-FoxO1-F, a VP16 fusion with a viral VP16 activation domain fused to the FoxO1 N-terminus, or pACT-FoxO1-R, a reverse oriented VP16- FoxO1) were also co-transfected. pcDNA-FLAG was used as a control. The cells were subsequently treated with rosiglitazone (1μM) or DMSO control for 24 h prior to

luciferase assay. Note that the rosiglitazone-induced PPARγ transactivation was inhibited by FoxO1, but enhanced by VP16-FoxO1, and this remarkable shift strongly suggests a direct interaction between PPARγ and FoxO1. *c*, Mammalian two-hybrid assays. HIRc-B cells were cotransfected with a DNA mixture consisting of 100 ng of pG5-Luc, 100 ng of VP16-FoxO1, and 100 ng of Gal4-hPPARγ2 and exposed to rosiglitazone (1μM) for 24 hours prior to luciferase assay. FoxO1 was fused to VP16 in either forward or reverse orientation (indicated as f or r). hPPARγ2 was fused to Gal4 in the same manner (indicated as F or R). Note that the VP16-FoxO1-F + Gal4-hPPARγ2-F resulted in a significantly enhanced reporter signal in comparison to other combinations. More importantly, the reporter was further activated when cells were treated with Rosiglitazone. *d*, Cells co-transfected in the same manner as panel *c* were subjected to sequential overnight starvation and insulin treatment before luciferase assay. ROSI, rosiglitazone; INS, insulin. Data are presented as the average ± SD. Letters above the bars show statistical groups (ANOVA, $p < 0.05$).

Supplemental Fig 4.

a, Transactivational function of FoxO1 was assayed in HEK293 cells by a luciferase reporter driven by a promoter containing three copies of the IGFBP1 insulin-responsive

sequence (IRS) (3×IRS-Luc). The DNA binding domain mutant FoxO1 showed no transactivational function, although it was transrepressionally competent. b, D10 3T3-L1 adipocytes were infected with adenovirus encoding either Δ256 truncated FoxO1 or GFP control, then starved in DMEM containing 0.1% BSA for 8 hours, followed by overnight incubation with 1μM Rosiglitazone or DMSO control in combination with 100 ng/ml insulin or PBS. Endogenous expression of Pepck mRNA was measured by real-time time PCR. c, D10 adipocytes were exposed to 1μM Rosiglitazone or DMSO control in combination with 100 ng/ml insulin or PBS as indicated. Duplicate plates of cells were pooled for each condition. Soluble chromatin was immunoprecipitated with anti-FoxO1 antibody. Enrichment of *Gpd1* PPRE-containing DNA sequences in the immunoprecipitated DNA pool over input control was quantified by real-time PCR. Numerical values above bars show relative copies. *d*, Primers designed for a control region (Rps3 promoter) without a PPRE sequence resulted in no amplification from immunoprecipitates. Data are presented as the average ± SD. Letters above the bars (*a* and *b*) show statistical groups (ANOVA, $p < 0.05$).

Supplemental Fig 5.

a, Amino acid sequence alignment of the putative domain that mediates FoxO1 transrepression among various species. Atypical LxxLL nuclear receptor box motifs are highlighted in red. *b*, Experiments similar to Fig 1B revealed that an internal deletion of aa358-363 (the first atypical LxxLL motif) does not affect the ability of FoxO1 to transrepress PPARγ. Protein loading was confirmed by immunoblotting. *c*, Similarly, point mutations of L374A/L375A or L379A/L380A did not affect the ability of FoxO1 to transrepress PPARγ.

Supplemental Fig 6.

a. Adipocytes were transduced with Ad-GFP, Ad-FoxO1-WT, Ad-FoxO1-CA or Ad-FoxO1-Δ256, and then subjected to sequential starvation and 16 hours of Rosiglitazone treatment; 10μM isoproterenol was then applied to stimulate lipolysis, and free fatty acid released to the culture medium was measured. The FFA concentration in the Ad-GFP group was set to 1. Comparable protein expression of FoxO1 mutants was confirmed (right panel) by western blot using an anti-HA probe. Data are presented as the average ± SD. Letters above the bars show statistical groups (ANOVA, $p < 0.05$). b. PPARγ mRNA expression in FoxO1 transduced fat cells. D10 3T3-L1 adipocytes were infected with adenovirus encoding either wild type, constitutively active mutant,

or GFP control, starved in DMEM containing 0.1% BSA for 8 hours, and then exposed overnight to 1μM Rosiglitazone or DMSO control in combination with 100 ng/ml insulin or PBS. Endogenous expression of PPARγ mRNA was assayed by real-time PCR. Note that FoxO1 decreases PPARγ mRNA levels, but insulin abolishes the FoxO1-WT inhibition. Rosiglitazone also decreases PPARγ mRNA significantly. FoxO1, which transrepresses PPARγ significantly in the presence of Rosiglitazone, does not further decrease the PPARγ mRNA.

Supplemental table 1

Target gene	Accession Number	Primer ID	sequences (5'-3')
target sequence of siRNA			
FoxO1	NM_019739.2	siFoxO1	GCA CCG ACT T TA TGA GCA ACC
primers used for ChIP assay			
Gpd1	NM_010271	forward	TTC CTG AAG CCT GGA AGG AG
		reverse	GCC AGC CTT GGT CTA CAG AG
Pepck	NM_011044	forward	GAACTCCGAC AAGCAAGCTC TCAGC
		reverse	CCCAAGTGTC TGGAGAAAGG ACG
Rps3	NM_012052	forward	CCAAATGGCCTTGAACTCACC
		reverse	ACCACATGGTGGTTCACAACC
primers used for real time PCR			
Rps3	NM_012052	forward	ATC AGA GAG TTG ACC GCA GTT G
		reverse	AAT GAA CCG AAG CAC ACC ATA G
Cap1	NM_009166	forward	GTGCTTAAGAGGCCATTGGTG
		reverse	TACCAAACTGCCTCGTCCTTC
Pparg	NM_011146	forward	CTG TCG GTT TCA GAA GTG CCT
		reverse	CCC AAA CCT GAT GGC ATT GTG AGA CA
Pepck	NM_011044	forward	GAGAGTCACCCCTTCCCACTCACAGC
		reverse	CAGAGACTATGCGGTGATTTCCCCTCC
glycerol kinase (GyK)	U48403	forward	GGAGACCAGCCCTGTTAAGCT
		reverse	GTCCACTGCTCCCACCAATG
Gpd1	NM_010271	forward	CTTTGCTCGAACTGGAAAGTC
		reverse	CATAGCACACTTTGTACACCG
FoxO1	NM_019739.2	forward	GGAATGACCTCATGGATGGAG
		reverse	GTGAAGGGCATCTTTGGACTG

Fan W, et al. Supplemental Fig. 1

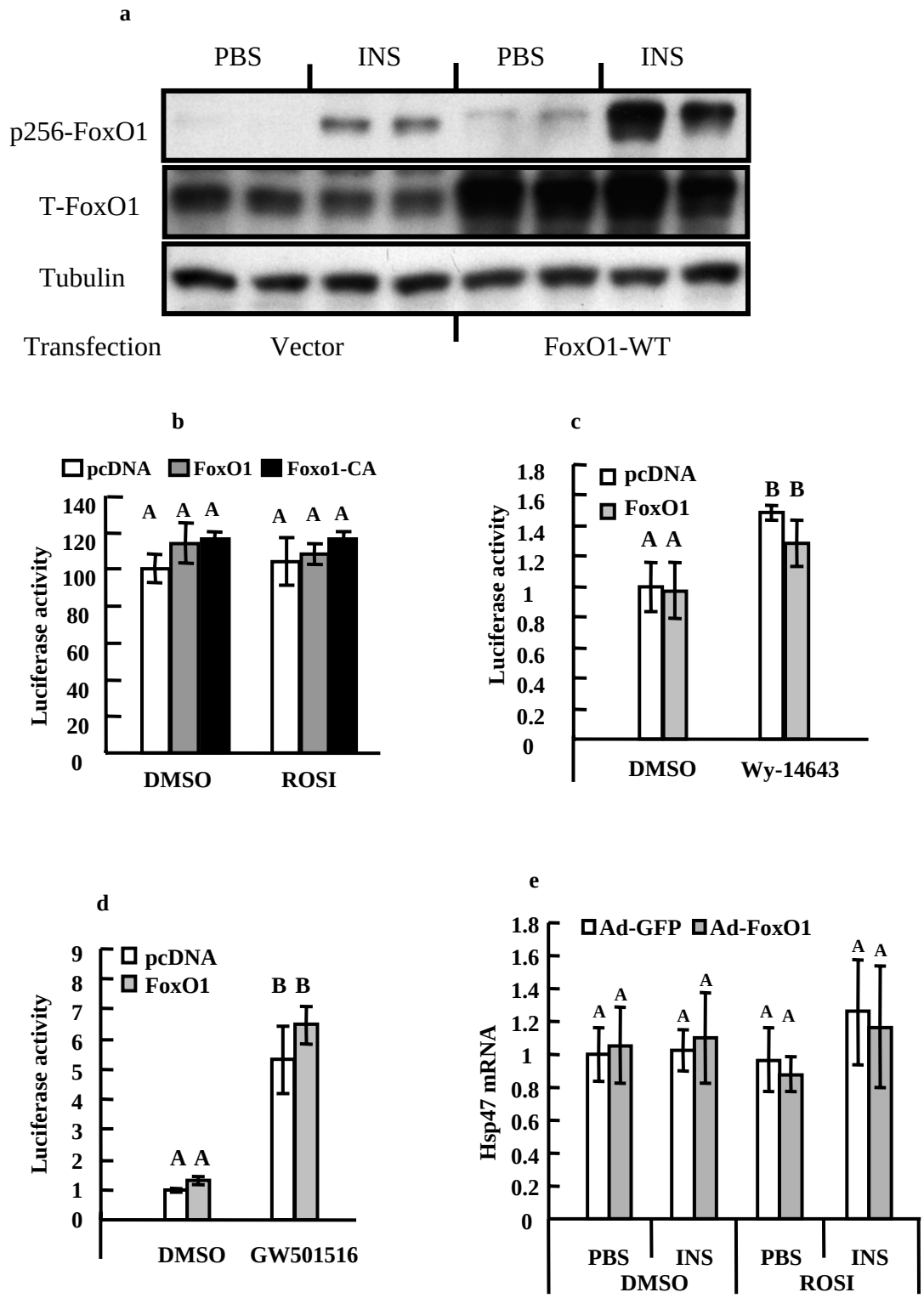

Fan W, et al. Supplemental Fig. 2

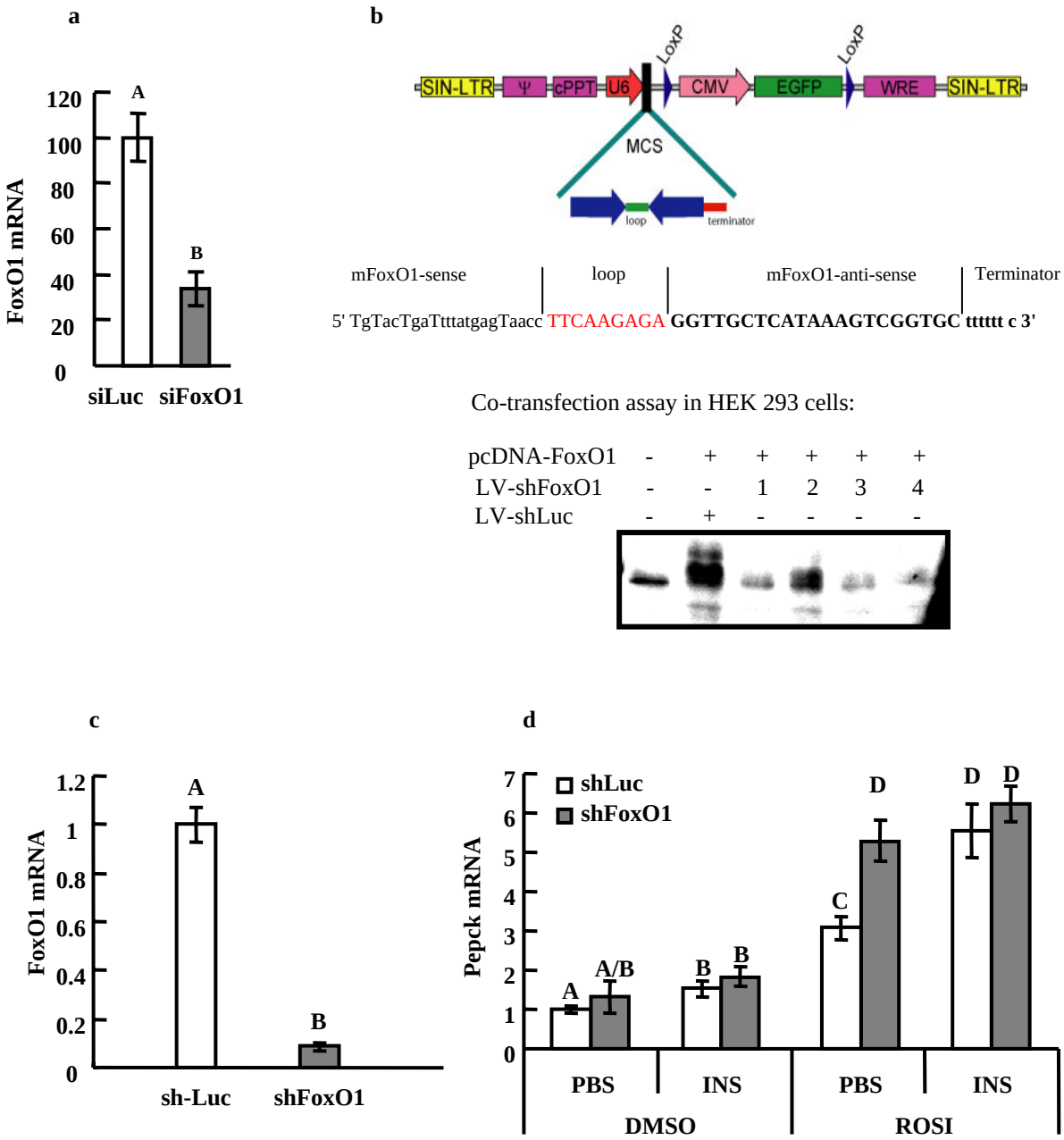

Fan W, et al. Supplemental Fig. 3

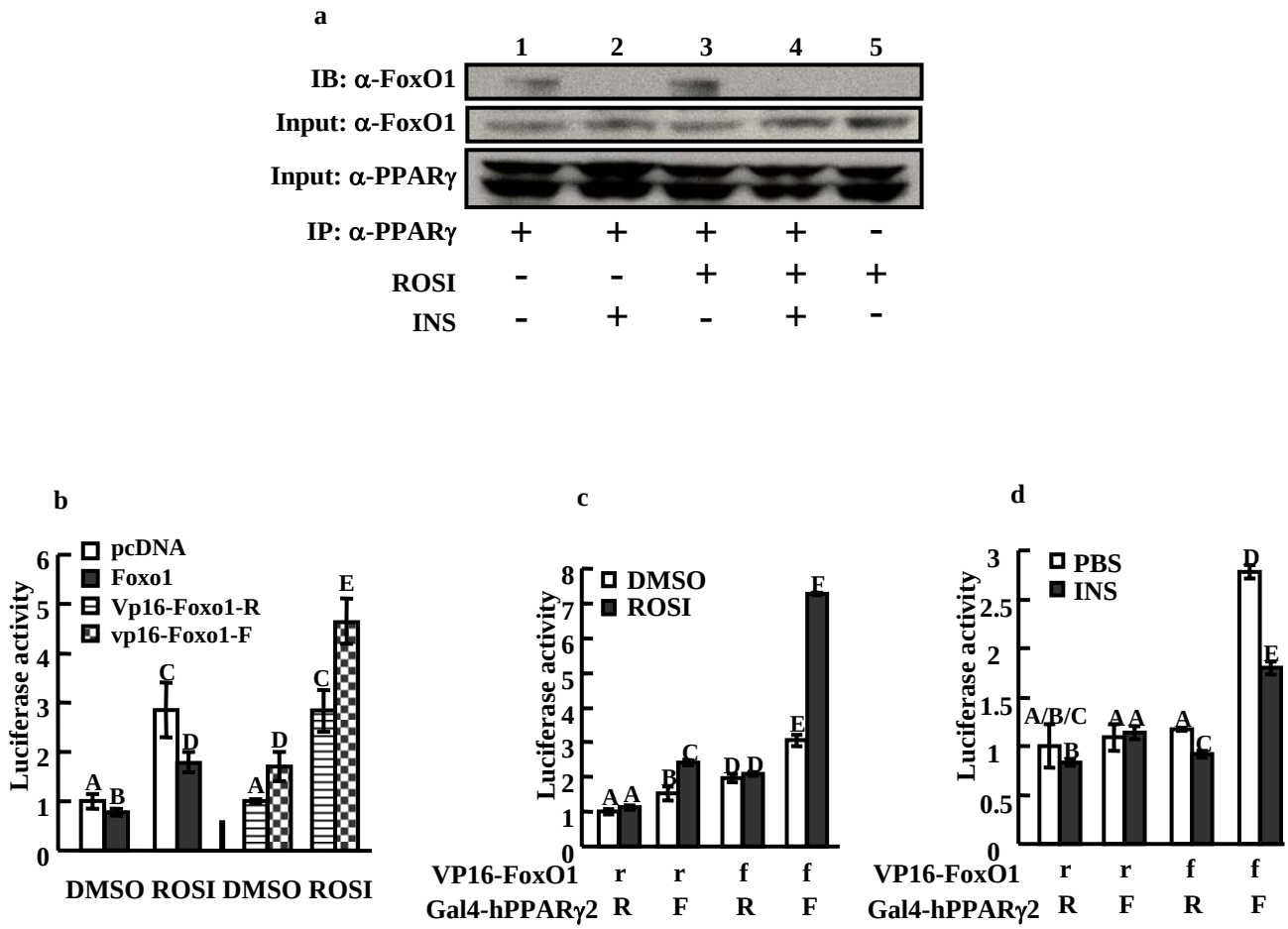

Fan W, et al. Supplemental Fig. 4

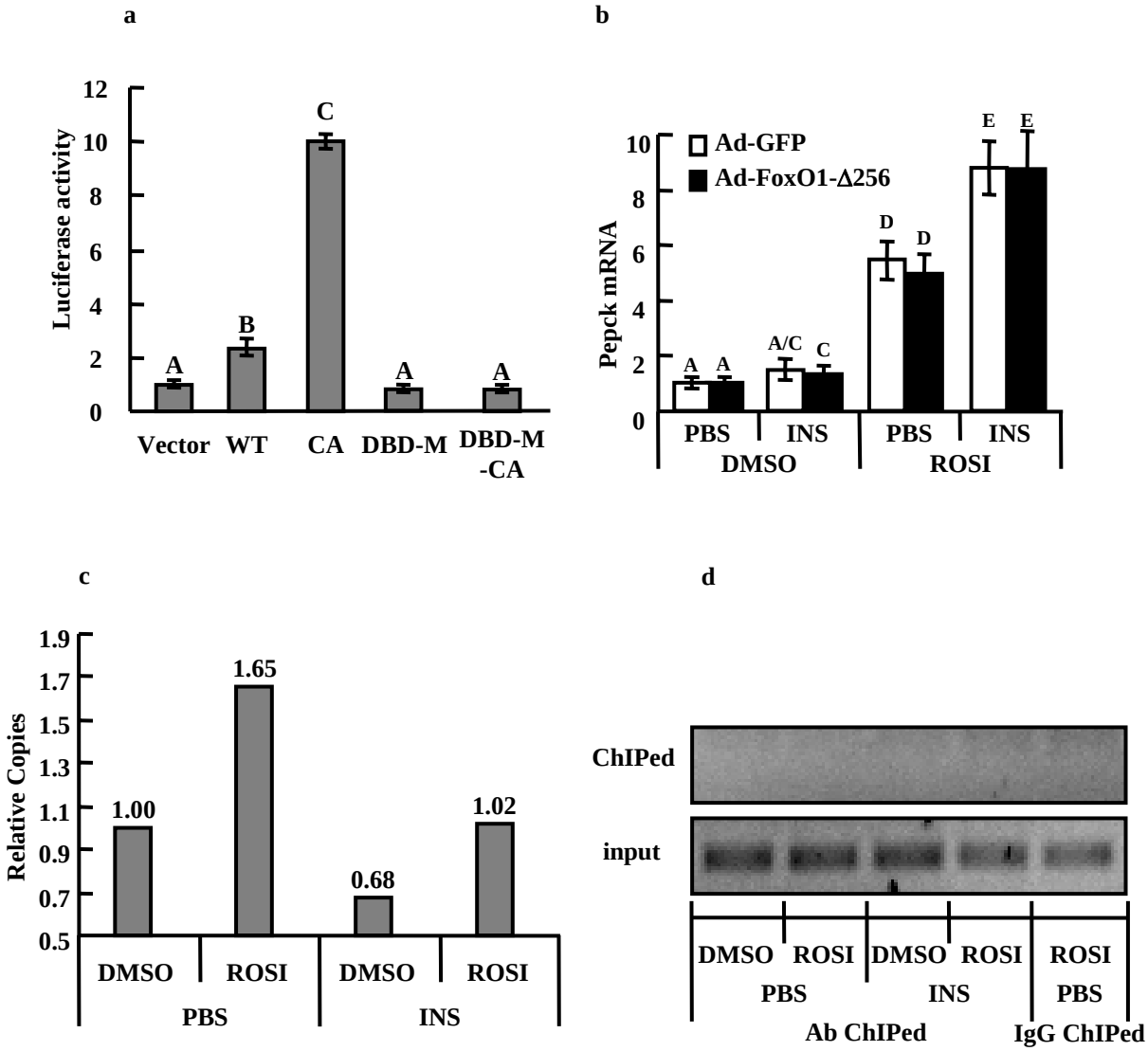

Fan W, et al. Supplemental Fig. 5

a: Amino acid sequences alignment

Mus musculus : 358LPSLSEISNPENMENLLDNLNLLSSPTSLTV388
Homo sapiens: LPSLSEISNPENMENLLDNLNLLSSPTSLTV
Danio rerio : LPSLSEMAGSLGHSGSENVMENLLDNLNLLSPKNPSTG
Xenopus tropicalis : LPSLSEMGNSENMENLLDNLNLLSPNTSTQS
Rattus norvegicus : LPSLSEISNPENMENLLD NLNLLSSPTS LTV
Sus scrofa : LPSLS EISNPENMEN LLDNLNLLSS PTSLTV
Xenopus laevis : LPS LSEMGNSENMENLLDNLNLL TPNSSTQS
Canis familiaris : LPS LSEISNPENMENLLDNLNLL SSPTPLTV
Pan troglodytes : LPSLSEISNPENMENLLD NLNLLSSPTS LTV
Macaca mulatta : LPSLSEISNPENMENLL DNLNLLSSPT SLTV

b

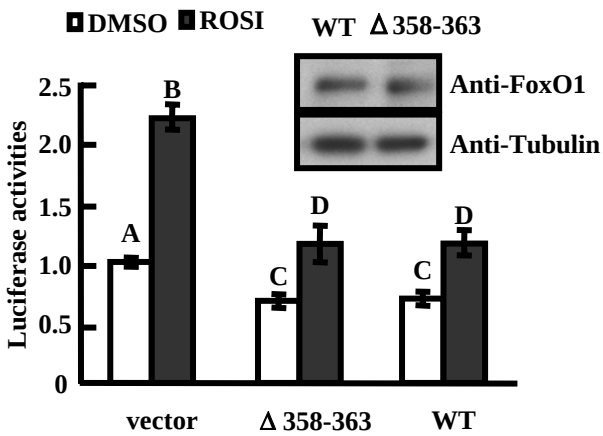

c

373LLDNLNLL380 → LLDNLNAA (L379A/L380A)
373LLDNLNLL380 → AADNLNLL (L373A/L374A)

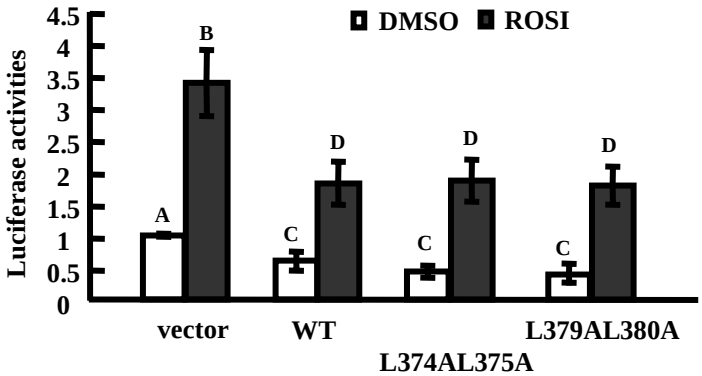

Fan W, et al. Supplemental Fig. 6